NATURAL HAZARDS RESEARCH PLATFORM

Kaikōura Earthquake Short-Term Project

Title: Post-seismic deformation following the Kaikōura earthquake

Leader: Sigrún Hreinsdóttir
Organisation: GNS Science
Total funding (GST ex): $75,000

Postseismic deformation following the Kaikōura Earthquake

S. Hreinsdóttir, N. Palmer, I. Hamling, L. Wallace, S. Ellis, P. Upton, R. Hart

Abstract

The 14 November 2016 (local time) Mw 7.8 Kaikōura earthquake in New Zealand ruptured at least 12 major crustal faults and caused widespread damage across the northern South Island. In immediate response to the earthquake 80 GPS sites were measured and several new continuous and semi continuous GPS stations were installed to augment the GeoNet/PostitioNZ CGPS network. This report documents work undertaken after the initial response phase. In March 2017 we went out and completed the measurements of the top of the South Island GPS network to set the groundwork for future postseismic studies in the region. In addition, we measured key sites around Arthur's Pass and serviced and downloaded data from semi continuous GPS stations. Available GPS data were analysed to study the early time dependent postseismic ground response following the earthquake. For a better spatial resolution, we acquired Sentinel-1 SAR satellite data and formed interferograms to evaluate the postseismic deformation. The first few months of GPS and InSAR measurements following the Kaikōura earthquake show large-scale northeast-directed displacements and uplift with the most rapid deformation observed in the region of Cape Campbell. The overall pattern of deformation suggests that the majority of deformation can be explained by slip on the underlying subduction interface, as well afterslip on the Needles fault and, to lesser extent, slip on the Kekerengu and Jordan fault.

1. Introduction

On 14 November 2016, the Kaikōura earthquake ruptured multiple faults in the South Island of New Zealand. The magnitude 7.8 earthquake was the largest to hit New Zealand since the M7.8 Dusky Sound earthquake in 2009 (Beavan et al., 2010) and is one of the most complex crustal earthquakes ever recorded, rupturing over 170 km, with significant slip along several crustal faults (Stirling et al., 2017, Hamling et al., 2017). In addition, the earthquake possibly ruptured portions of the southern Hikurangi subduction plate interface beneath the northern South Island (Hamling et al., 2017; Duputel et al., 2017; Bai et al., 2017).

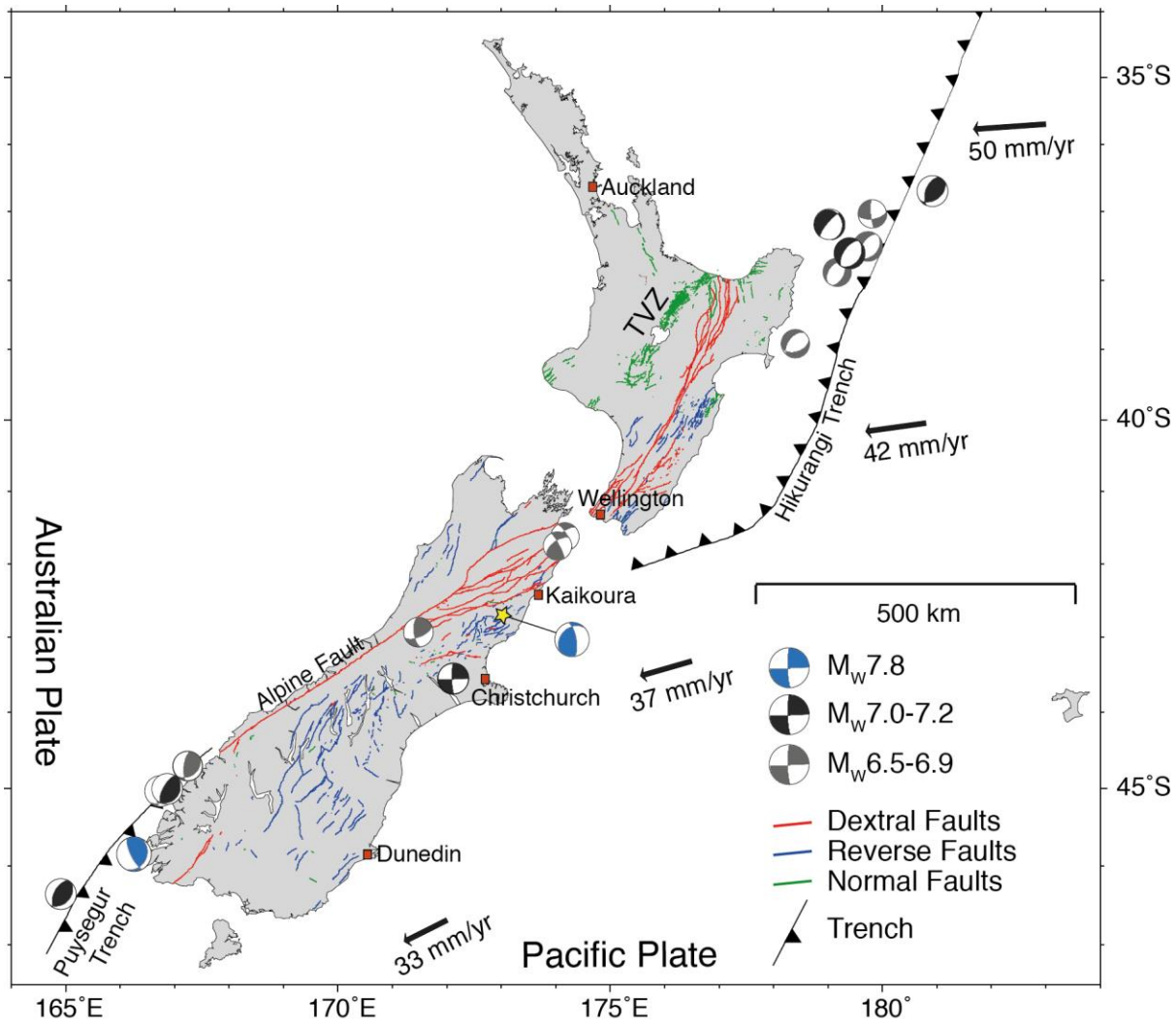

Figure 1. The Kaikōura earthquake (star) initiated in the North Canterbury region and ruptured northeast along multiple crustal faults. Focal mechanism from the CMT catalogue spanning 1990 to 2017 (Ekström et al., 2012; Dziewonski et al., 1981), faults from the NZ fault database (Langridge et al., 2016).

In the weeks following the Kaikōura earthquake over 80 existing GPS sites, mostly located within 50 km of the fault ruptures, were measured, augmenting the sparse continuous GPS network in the region (Hamling et al., 2017). In addition, synthetic Aperture Radar (SAR) satellite data from the

Sentinel-1A (European space agency) and ALOS-2 (Japanese space agency) missions were acquired. Analysis of the GPS data and the SAR interferograms (InSAR) reveals complex faulting and block movements in the northern Canterbury fault zone and the Marlborough fault system. Modelling of the geodetic and coastal uplift data (Hamling et al., 2017, Clark et al., 2017) suggests significant faulting on at least 12 major faults, both onshore and off, with maximum surface offsets of 12 m along the Kekerengu fault, in general agreement with field observations. The majority of the observed deformation can be explained by rupture along crustal faults (Hamling et al., 2017). However, observed inland subsidence suggests up to 1-2 metre of slip along the deeper portion of the southern part of the Hikurangi plate interface (Clark et al., 2017).

Postseismic deformation from an event of this magnitude (Mw 7.8) will affect the region for years with afterslip on crustal faults, viscoelastic response of the mantle and possibly slip on the underlying subduction interface. Afterslip is aseismic slip, very similar to creep, that takes place along the faults that ruptured during an earthquake and dominates near field motions for weeks to months, whereas viscoelastic is the response of the lower crust and upper mantle to the earthquake and dominates in longer term and affects a wider region. These movements (afterslip, viscoelastic) will not be perceptible by people at the surface, but are measureable with the GPS data that provides insight into the nature of the crust. Importantly, we can only detect or measure these movements after large earthquakes, hence the time critical factor in our field campaign.

It is critical to better understand the sources of the observed postseismic deformation to inform hazard assessment for regional faults and the subduction zone.
The main aim of this work was to

1) Complete the measurements of the GPS network in the northern South Island to set the basis for long-term postseismic studies of the region.
2) Operate semi continuous GPS stations to improve the spatial distribution of continuous measurements for studying the time varying deformation following the earthquake.
3) Analyse and model GPS and InSAR data to inform seismic hazard assessment for the region.

2. Measurements

Prior to the Kaikōura earthquake, 15 GeoNet/PositioNZ GPS stations were operating in the top of the South Island (TOPS, north of 43˚S, Figure 2). In addition, one IGS station is located in Marlborough and a handful of GPS reference stations are operated in the region by NZ geospatial and surveying firms. Within 24 hours of the earthquake, GeoNet finalized the installation of a new GPS site in Seddon (SEDD). In the next five days, GeoNet set up and started logging data at six additional temporary monuments (LRR1, WRA1, LOK1, TEN2, GDS1, and MUL1) which were a few months later replaced by five permanent stations (CLRR, WRAU, GLOK, TENN and LOOK to replace both GDS1 and MUL1).

Over 80 GPS sites in the TOPS campaign GPS network were measured in a rapid response to the earthquake in collaboration between GNS Science, Otago University and LINZ. The sites logged data for a minimum of two days and up to two weeks each. Eight existing sites with permanent monuments were set up for semi continuous observations (ADJ4, A5AF, BLBH, A7R5, 1163, A6NF, B23Y and A8HB*). In addition, GNS Science and Otago University installed eight new monuments for semi continuous operation (EXA6, EXA7, EXA8, EXA9, EX6B, EX6C, EX6D, EX6E). One additional semi continuous site was installed in Arthur's Pass (EXFV) in response to increased seismic activity following the Kaikōura earthquake (Table 1).

The semi continuous sites have been visited a few times to check on equipment and power and download data. A couple of sites have had faulty solar panels which have since been replaced, causing large data gaps. One setup, with receiver, antenna and power setup from Otago University was stolen before any data was retrieved (A8HB). The data from semi continuous site in Kaikōura (1163) has benefited surveyors working in the region due to damaged infrastructures. We have benefitted from that collaboration by having data downloaded and the site inspected.

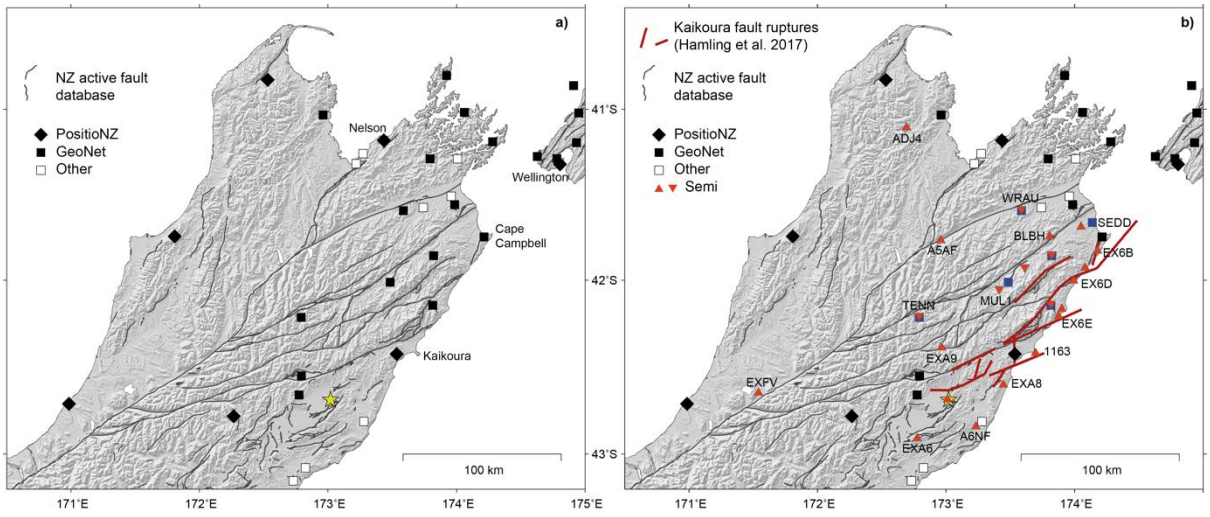

Figure 2. a) The continuous GPS network at the top of the South Island prior to the Kaikōura earthquake (star), was relatively sparse. b) In the weeks to months following the earthquake GeoNet, University of Otago and GNS science installed a few continuous (blue squares) and semi continuous (red triangles) sites to measure postseismic deformation due to the earthquake. Inverted triangles show semi continuous sites that are being replaced by permanent GPS stations.

In March 2017, 48 sites were measured in the TOPS campaign network and Arthur's Pass region (Figure 3, Table 2), completing the post-earthquake measurements for the area (last measured in 2012) and laying the groundwork for future long-term postseismic deformation studies. Many of the sites in the TOPS network are helicopter access only due to the remoteness of the sites, and others were inaccessible by car during the field season due to road closures following the earthquake. A handful of sites could not be reached or were destroyed in the earthquake.

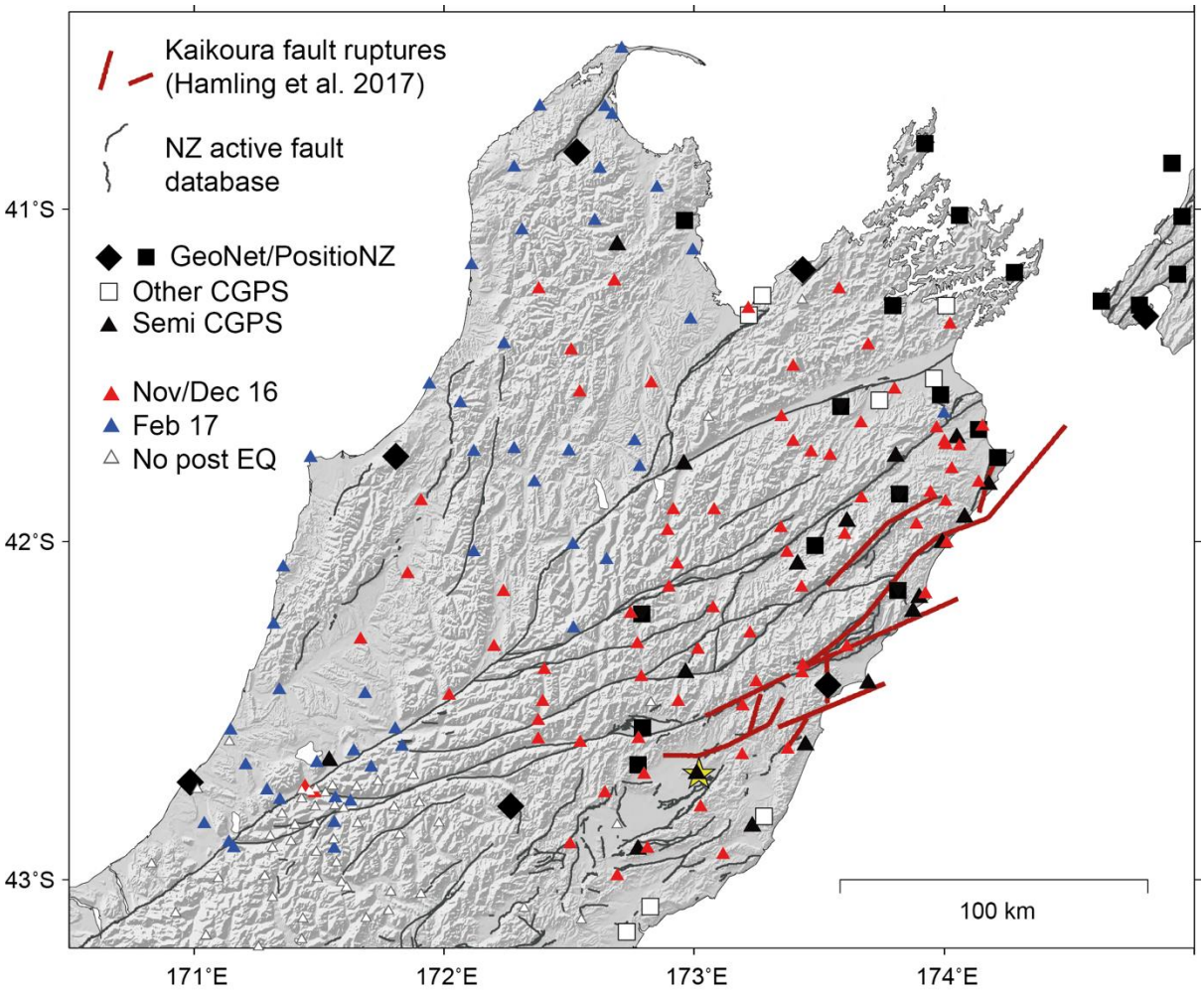

Figure 3. GPS measurements of the TOPS campaign GPS network following the Kaikōura earthquake. The red sites were measured within a few weeks of the earthquake whereas blue sites were measured in February 2017. Yellow star shows the epicentre and red thick lines fault rupture model by Hamling et al. (2017).

To compliment the GPS data, we use Synthetic Aperture Radar (SAR) satellite data acquired every 6-12 days by Sentinel-1, the European (ESA) Space Agency mission. InSAR measurements give a better spatial coverage than GPS but only measure the movement away and toward the satellite. The descending satellite pass has a more favourable look angle to the post earthquake deformation field, giving a better signal to noise ratio. We use descending SAR images from 16 November, 16 December and 4 March to evaluate the postseismic deformation during the first four months following the Kaikōura earthquake.

3. Key findings

The Kaikōura earthquake ruptured within a complex tectonic region of the northern South Island, where we see transition from subduction at the Hikurangi subduction zone (North Island) to strike-slip and collision along the Alpine Fault in the central South Island (Wallace et al., 2012). A majority of the coseismic deformation can be explained by rupture of upper crustal faults in Canterbury fault zone and the Marlborough fault system with the largest moment release taking place on the Jordan thrust fault -Kekerengu dextral strike-slip segment.

The GPS measurements following the earthquake show variable postseismic deformation in the region (Figure 4), with the most rapid movement at sites in the Cape Campbell region, moving toward northeast and up (Figure 5), coinciding with a large cluster of aftershocks. Sites along the east coast have a more east-southeast movement toward the coast, but sites in the epicentral region show relatively minor postseismic response. (Figure 4,5). We see significant postseismic deformation over 100 km from the fault rupture, with sites on the west coast moving a few cm toward the southwest, toward the Kaikōura region, and sites in the North Island moving northeast, away from the Kaikōura region.

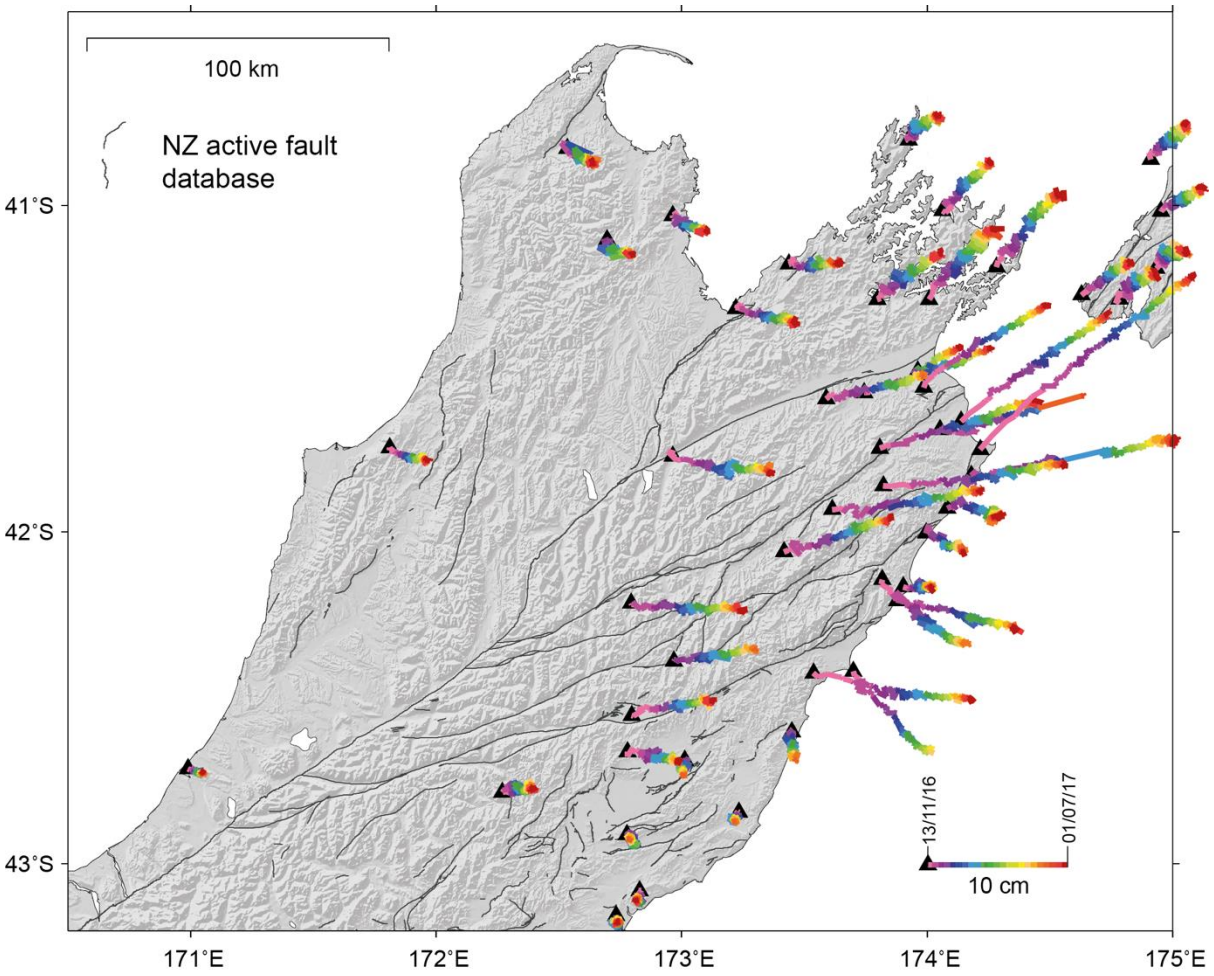

Figure 4. Horizontal movement at continuous GPS and semi continuous GPS stations from 13 November 2016 to 01 July 2017 UTC following the Kaikōura earthquake. The colour code indicates time of movement and length reflects how much it moved (see scale in lower right corner). Several

sites are missing the first few days of postseismic movement, reflecting their installation date a few days after the earthquake.

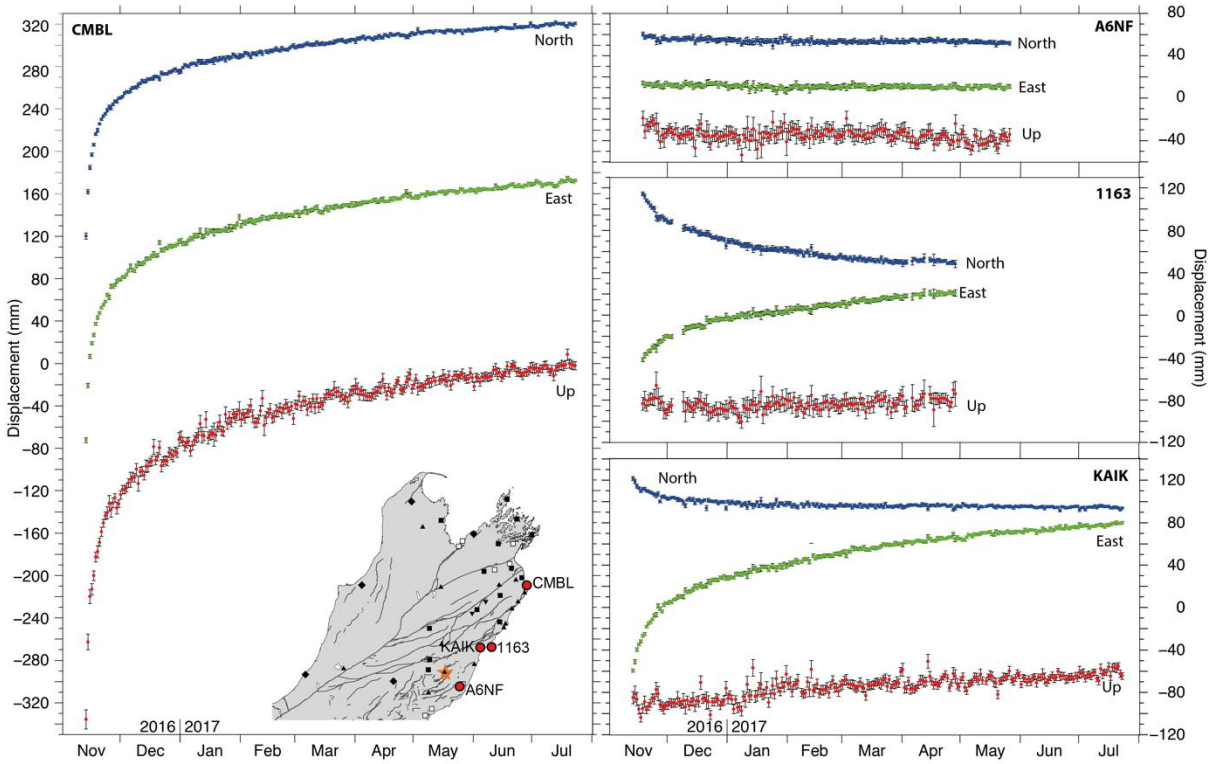

Figure 5. Time series for semi and continuous GPS sites CMBL, KAIK, 1163 and A6NF. The site closest to the epicentre (A6NF) has minor movement following the earthquake where as CGPS site CMBL moves over 330 mm up and 313 mm towards northeast from 13 November 2016 to 1 July 2017.
Continuous sites capture the first days of the deformation (e.g. KAIK) whereas semi continuous sites Installed a few days after the earthquake missed the first few days of rapid movement (e.g. 1163).

The InSAR measurements show large-scale northeast-directed displacements, with the largest movement in the Cape Campbell region in agreement with the GPS data, suggesting significant afterslip on the Needles fault. The GPS and InSAR data also reveal a large uplift/subsidence pair (Figure 6) which is not easily explained by afterslip on crustal faults that ruptured during the earthquake. The overall pattern and scale of post-earthquake deformation is more consistent with slip on a low-angle source at depth, such as the subduction interface beneath the northern South Island (Wallace et al., submitted, Hreinsdottir et al., 2017). Modelling of the InSAR and GPS data suggest up to 0.5 m of slip on the subduction plate interface beneath the northern South Island, in addition to up to 0.5 m of afterslip on the Needles fault, and significant slip on the Kekerengu and Jordan fault (Hreinsdottir et al., in prep, Wallace et al., submitted). The afterslip distribution on the plate interface has also been used to inform the change in nearer-term hazard posed by the Hikurangi subduction zone, following triggering of unprecedented, large-scale slow slip events after the Kaikōura earthquake. This was presented and discussed at an international expert elicitation workshop to redefine the hazard forecasts for central New Zealand over the next 1-10 years. The updated hazard forecasts can be found here:
http://www.geonet.org.nz/news/5JBSbLk9qw8OU4uWeI86KG.

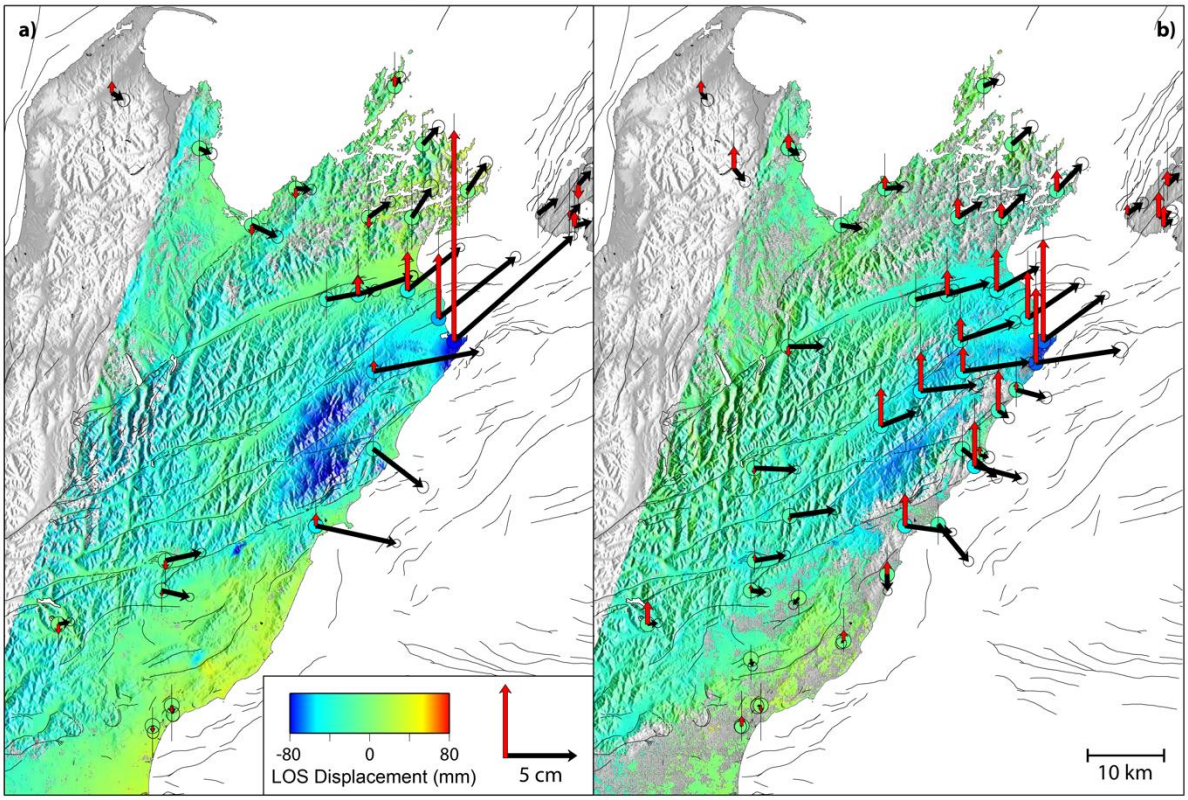

Figure 6. InSAR (line of sight) and GPS observations (red-vertical, black-horizontal) spanning a) 16 November to 16 December 2016 and b) 16 December 2016 to 4 March 2017. Large uplift signal is observed in the northeast South Island where as inland sites are subsiding.

4. Future work

Postseismic processes following the Kaikōura earthquake will to continue to affect the deformation in the region for years. It is likely that longer-term viscoelastic transients are currently embedded in the deformation signal. Measurements spanning a longer time period are needed to disentangle the afterslip vs. viscoelastic deformation components. In January/February 2018 we will re measure the TOPS GPS network as part of a EQC funded project (PI Hreinsdottir) to evaluate the first 15 months of postseismic deformation following the earthquake. We plan to continue to run key semi continuous stations in the region, depending on equipment and funding availability. The TOPS GPS network is scheduled to be measured again in January 2020 as part of the SSIF funded project "Tectonics and Structure of Zealandia".

5. Acknowledgements

The GPS measurements following the Kaikōura earthquake have been a collaborative effort between GNS Science, LINZ and Otago University of Surveying. Students from Victoria University of Wellington and University of Texas at Austin participated in the measurements. Continuous GPS data are available from the GeoNet and PositioNZ networks. AllTerra and Global Survey have generously given us access to GPS data from continuous GPS stations they operate in the region.

6. References

Bai, Y., Lay, T., Cheung, K. F., & Ye, L. (2017). Two regions of seafloor deformation generated the tsunami for the 13 November 2016, Kaikōura, New Zealand earthquake. *Geophysical Research Letters, 44*: 6597–6606, doi:10.1002/2017GL073717.

Beavan, J., Samsonov, S., Denys, P., Sutherland, R., Palmer, N., & Denham, M. (2010). Oblique slip on the Puysegur subduction interface in the 2009 July Mw 7.8 Dusky Sound earthquake from GPS and InSAR observations: Implications for the tectonics of southwestern New Zealand. *Geophysical Journal International*, *183*(3), 1265-1286.

Clark, K.J., Nissen, E.K., Howarth, J.D., Hamling, I.J., Mountjoy, J.J., Ries, W.F., Jones, K.E., Goldstein, S., Cochran, U.A., Villamor, P., Hreinsdottir, S., Litchfield, N.J., Mueller, C., Berryman, K.R., & Strong, D.T. (2017). Highly variable coastal deformation in the 2016 M_W7.8 Kaikōura earthquake reflects rupture complexity along a transpressional plate boundary. *Earth and Planetary Science Letters, 474:* 334-344; doi: 10.1016/j.epsl.2017.06.048

Duputel, Z., & Rivera, L. (2017). Long-period analysis of the 2016 Kaikōura earthquake. *Physics of the Earth and Planetary Interiors*, *265*: 62-66; doi:10.1016/j.pepi.2017.02.004

Dziewonski, A. M.,. Chou, T.-A., &. Woodhouse, J.H., (1981). Determination of earthquake source parameters from waveform data for studies of global and regional seismicity. *Journal of Geophysical Research: Solid Earth*, 86, 2825-2852. doi:10.1029/JB086iB04p02825

Ekström, G., Nettles, M., & Dziewonski, A.M., (2012). The global CMT project 2004-2010: Centroid-moment tensors for 13,017 earthquakes. *Physics of the Earth and Planetary Interiors*, 200-201, 1-9. doi:10.1016/j.pepi.2012.04.002

Hamling, I. J., Hreinsdóttir, S., Clark, K., Elliott, J., Liang, C., Fielding, E., ... & D'Anastasio, E., (2017). Complex multifault rupture during the 2016 Mw 7.8 Kaikōura earthquake, New Zealand. *Science*, *356*(6334), eaam7194.

Hreinsdóttir, S., Hamling, I., Ellis, S., Wallace, L., Denys, P., Palmer, N., … & D'Anastasio, E., (2017). Postseismic deformation following the 2016 Mw 7.8 Kaikōura earthquake, New Zealand. IN: *IAG-IASPEI, July 30-August 14, 2017, Kobe, Japan: Joint Scientific Assembly of the International Association of Geodesy and the International Association of Seismology and Physics of the Earth's Interior*

Langridge, R.M., Ries W.F., Litchfield, N.J., Villamor, P., Van Dissen, R.J., Barrell, D.J.A., Rattenbury, M.S., Heron, D.W., Haubrock, S., Townsend, D.B. Lee, J.M., Berryman, K.R., Nicol, A., Cox, S.C., & Stirling, M.W. (2016). The New Zealand Active Faults Database. *New Zealand Journal of Geology and Geophysics, 59(1): 86-96.*

Stirling, M. W., Litchfield, N. J., Villamor, P., Van Dissen, R. J., Nicol, A., Pettinga, J., ... & Mountjoy, J. (2017). The Mw 7.8 2016 Kaikōura earthquake: Surface fault rupture and seismic hazard context. *Bulletin of the New Zealand Society for Earthquake Engineering.*, (2), 73-84.

Wallace, L.M., Barnes, P., Beavan, R.J., Van Dissen, R.J., Litchfield, N.J., Mountjoy, J., Langridge, R., Lamarche, G., & Pondard, N., (2012). The kinematics of a transition from subduction to strike-slip: an example from the central New Zealand plate boundary. J*ournal of Geophysical Research: Solid Earth*, *117(2):* B02405. Doi:1029/2011JB008640

Wallace, L.M., Hreinsdottir, S., Ellis, S., Hamling, I., D'Anastasio, E., Denys, P., Triggered slow slip and afterslip on the southern Hikurangi subduction zone following the Kaikōura earthquake, submitted to Geophysical Research Letters 2018.

Tables

Table 1. Temporary (semi) and continuous GPS stations in the South Island of New Zealand, north of 43˚S. Start date for continuous measurements are given for stations first operated following the Kaikōura earthquake, given in day of 2016 unless otherwise noted.

SITE	NAME	Operated by		Start date
1163	REF KA KAIKOURA PENINSULA	GNS Science	Semi CGPS	323
A5AF	TOP 1	GNS Science	Semi CGPS	322
A6NF	J MCCLURE	OUSD	Semi CGPS	323
A7R5	R STAR HILL	GNS Science	Semi CGPS	323
ADJ4	WN 114 COBB	GNS Science	Semi CGPS	336
B23Y	REF PATUTU	GNS Science	Semi CGPS	325
BLBH	BLACK BIRCH GPS	GNS Science	Semi CGPS	322
EX6B	CHANCET	GNS Science	Semi CGPS	326
EX6C	WHARANUI	GNS Science	Semi CGPS	330
EX6D	VALHALLA	GNS Science	Semi CGPS	327
EX6E	WAIPAPA BOAT COMPOUND	GNS Science	Semi CGPS	327
EXA6	OLD MT ALEXANDER RD SUMMIT	OUSD	Semi CGPS	333
EXA7	ISOLATED HILL NO 2	OUSD	Semi CGPS	334
EXA8	MT GUARDIAN STATION	OUSD	Semi CGPS	334
EXA9	ACHERON CONFLUENCE	OUSD	Semi CGPS	335
EXFV	EXFV	OUSD/GNS	Semi CGPS	345
GDS1	Gladstone Station	GeoNet	Semi CGPS	322
LOK1 GLOK	Glen Orkney Station	GeoNet GeoNet	Semi CGPS CGPS	321 164 2017
LOOK	Mount Lookout	GeoNet	CGPS	172 2017
LRR1 CLRR	Clarence River	GeoNet GeoNet	Semi CGPS CGPS	320 110 2017
MUL1	Muller Station	GeoNet	Semi CGPS	322
SEDD	Seddon	GeoNet	CGPS	319
TEN2 TENN	Lake Tennyson	GeoNet GeoNet	Semi CGPS CGPS	323 319 2017
WRA1 WRAU	Wairau Valley	GeoNet GeoNet	Semi CGPS CGPS	321 109 2017
CMBL	Cape Campbell	GeoNet	CGPS	
DURV	D'Urville	GeoNet	CGPS	

GLDB	Golden Bay	PositioNZ	CGPS	
HANM	Hanmer Basin	GeoNet	CGPS	
HOKI	Hokitika Airport	PositioNZ	CGPS	
KAIK	Kaikoura	PositioNZ	CGPS	
LKTA	Lake Taylor	PositioNZ	CGPS	
MAHA	Mahakipawa Hill	GeoNet	CGPS	
MRBL	Marble Point	GeoNet	CGPS	
NLSN	Nelson	PositioNZ	CGPS	
OKOH	Okoha	GeoNet	CGPS	
TKHL	Takaka Hill	GeoNet	CGPS	
TORY	Arapawa No. 2	GeoNet	CGPS	
WEST	Westport	PositioNZ	CGPS	
WITH	Wither Hills	GeoNet	CGPS	
MRL1	Marlborough 1	IGS	CGPS	
GSAM	Amberly	Global Survey	CGPS	
GSCV	Cheviot	Global Survey	CGPS	
GSBN	Blenheim	Global Survey	CGPS	
GSNL	Nelson	Global Survey	CGPS	
VPCT	Picton	AllTerra	CGPS	
VMCS	Mt Cass	AllTerra	CGPS	

Table 2. GPS sites observed in February 2017 with the support of this NHRP project. The First and Last columns show first and last day of measurements, in day of year.

Site	Latitude (˚)	Longitude (˚)	Height (m)	First	Last
1175	-42.02947	172.11845	1656.0	059	064
1181	-41.72908	172.49952	1486.6	053	057
1182	-41.72168	172.27987	1376.1	059	064
1186	-41.69859	172.76218	874.0	051	055
1188	-41.61583	173.99765	657.5	047	047
1204	-41.33304	172.98451	385.4	054	057
1432	-41.58349	172.06346	1476.0	059	064
1433	-41.72940	172.11726	1402.8	059	064
3662	-42.00844	172.51588	423.1	053	056
5112	-42.90779	171.55927	937.4	058	060
5116	-42.83188	171.56113	409.9	058	060
5118	-42.76934	171.62438	277.2	054	056
5119	-42.75919	171.56509	228.1	055	057
5122	-42.73616	171.29120	90.7	055	057
5123	-42.66190	171.20583	144.4	056	058
6754	-42.25689	172.51803	2248.6	059	064
6776	-41.74915	171.46616	74.4	053	056

6784	-42.45046	171.68336	267.5	053	056
6790	-42.55527	171.80430	179.5	053	056
A4UH	-40.87259	172.28044	891.0	054	057
A593	-40.87670	172.62134	1525.3	054	057
A598	-40.93421	172.85037	883.5	053	057
A6JU	-41.40595	172.23910	1383.3	059	064
A6M0	-41.03485	172.60308	1878.8	054	057
A70X	-40.71318	172.67200	165.8	051	056
A8JE	-42.55824	171.14449	75.2	057	059
A8KE	-42.65486	171.49153	1214.0	060	064
AC7G	-40.51200	172.70979	92.6	052	055
AC7M	-40.68794	172.38345	72.9	052	055
AC7W	-41.16836	172.10806	26.8	053	055
AC8P	-41.52821	171.94205	22.8	053	056
ACQY	-42.07520	171.35509	127.6	053	061
ADQ1	-42.24550	171.31711	33.8	056	058
ADTF	-41.77595	172.78196	582	053	054
AHM8	-41.12380	172.99448	25.7	054	058
AHNG	-42.76425	171.34210	115.5	054	057
AM7G	-40.68913	172.64278	69.5	052	055
B1TF	-41.06282	172.31123	1663.9	054	054
B29N	-42.61958	171.63766	1174.8	060	065
B2BH	-42.43908	171.33946	73.2	059	061
B2L2	-42.83505	171.04106	33.7	059	060
B3JU	-41.80680	172.34022	198.5	060	064
B9EW	-42.90532	171.15791	114.5	059	062
C8UB	-42.64934	171.54053	129.7	058	060
DK0M	-42.66872	171.70768	1267.5	060	063
DK0R	-42.60734	171.83181	1065.0	060	064
DN4J	-42.05316	172.65000	1425.0	059	064
EBVN	-42.88890	171.13766	82.3	059	061